

# Role of buoyancy-driven vortices in inducing different modes of coupled behaviour in candle-flame oscillators

Cite as: AIP Advances 9, 015119 (2019); <https://doi.org/10.1063/1.5078674>

Submitted: 27 October 2018 . Accepted: 07 January 2019 . Published Online: 16 January 2019

Suraj Dange , Samadhan A. Pawar , Krishna Manoj, and R. I. Sujith

## COLLECTIONS

Paper published as part of the special topic on [Chemical Physics](#), [Energy, Fluids and Plasmas](#), [Materials Science](#) and [Mathematical Physics](#)



View Online



Export Citation



CrossMark

## ARTICLES YOU MAY BE INTERESTED IN

[Oscillation quenching and phase-flip bifurcation in coupled thermoacoustic systems](#)

Chaos: An Interdisciplinary Journal of Nonlinear Science **29**, 093135 (2019); <https://doi.org/10.1063/1.5114695>

[Coupled interaction between unsteady flame dynamics and acoustic field in a turbulent combustor](#)

Chaos: An Interdisciplinary Journal of Nonlinear Science **28**, 113111 (2018); <https://doi.org/10.1063/1.5052210>

[Effect of noise amplification during the transition to amplitude death in coupled thermoacoustic oscillators](#)

Chaos: An Interdisciplinary Journal of Nonlinear Science **28**, 093116 (2018); <https://doi.org/10.1063/1.5040561>



## NEW: TOPIC ALERTS

Explore the latest discoveries in your field of research

**SIGN UP TODAY!**

# Role of buoyancy-driven vortices in inducing different modes of coupled behaviour in candle-flame oscillators

Cite as: AIP Advances 9, 015119 (2019); doi: 10.1063/1.5078674

Submitted: 27 October 2018 • Accepted: 7 January 2019 •

Published Online: 16 January 2019



View Online



Export Citation



CrossMark

Suraj Dange,  Samadhan A. Pawar,  Krishna Manoj, and R. I. Sujith

## AFFILIATIONS

Department of Aerospace Engineering, Indian Institute of Technology Madras, Chennai 600036, India

<sup>a)</sup> Author to whom correspondence should be addressed. Electronic mail: [smadhanpawar@gmail.com](mailto:smadhanpawar@gmail.com)

## ABSTRACT

We investigate the coupled behaviour of two oscillatory flames produced by separate bundles of candles, referred to as candle-flame oscillators, as the distance between them is varied. Each bundle consists of four candles whose individual flames are fused so that the resultant flame produces self-sustained limit cycle oscillations. The recent study by Manoj *et al.* [Scientific Reports 8, 11626 (2018)] has reported the occurrence of four different modes of coupled behaviour, which include in-phase synchronization, amplitude death, anti-phase synchronization, and desynchronization by observing the flame dynamics of such coupled candle-flame oscillators. Here, we investigate the physical mechanism behind the occurrence of these different dynamical modes. Towards this purpose, we perform simultaneous measurements of the flow field around the candle flames using high-speed shadowgraph and of the reaction zone of each flame using high-speed CH<sup>\*</sup> chemiluminescence imaging. We notice that these modes are distinguished by the distinct features of the flame dynamics and the corresponding buoyancy-induced flows surrounding the flames. We observe that the difference in the interaction of vortices, formed due to the instability of buoyancy-induced flows around each flame at various distances, plays a significant role in inducing different modes of coupled dynamics between the oscillators. Furthermore, we find that the change in the length scales of vortices shed around the flames is a contributing factor in increasing the frequency of the oscillators during the transition from in-phase to anti-phase mode of synchronization.

© 2019 Author(s). All article content, except where otherwise noted, is licensed under a Creative Commons Attribution (CC BY) license (<http://creativecommons.org/licenses/by/4.0/>). <https://doi.org/10.1063/1.5078674>

## I. INTRODUCTION

Diffusion flames are known to oscillate at low frequencies, typically in the range of 10 to 20 Hz.<sup>1-4</sup> The oscillations in such flames are the result of the instability of the buoyancy-induced flow surrounding the flame.<sup>5</sup> The difference between the velocities of the buoyancy-induced hot flow and the stationary ambient air sets up an unstable shear layer, which then rolls up into spirals, leading to the formation of toroidal vortices around the flame surface. The sequential shedding of these vortices leading to the periodic elongation and contraction of the flame surface gives rise to low-frequency oscillations in diffusion flames.<sup>6</sup>

A candle flame is a familiar example among various diffusion flames. The oscillations in the flame of a single candle

are transient, sometimes referred to as flickering.<sup>7</sup> However, when three or more candles are bundled together, and their flames fused such that they form a single compound flame, the resulting large flame exhibits self-sustained periodic (or limit cycle) oscillations having a frequency in the range of 9 Hz to 13 Hz.<sup>8-10</sup> Such an arrangement of candles which produces oscillations in the flame is named as a candle-flame oscillator.

Various researchers have studied the reasons behind the self-sustained behaviour of a candle-flame oscillator. Kitahata *et al.*<sup>8</sup> theorized that the flame oscillations are the result of limited oxygen supply to the flame. In another study, Nagamine *et al.*<sup>11</sup> observed a descending flow of cold paraffin vapours just above the flame during the onset of oscillations and hypothesized about its role in inducing the flame

oscillations. The study by Okamoto *et al.*<sup>9</sup> speculated the generation of vortices around the luminous flame which gives rise to oscillations in the flame of a single candle-flame oscillator. Further, the authors conjectured that these vortices continuously move upward due to which the shape of the flame repeatedly expands and contracts. A similar conjecture was put forth in the numerical study by Yang *et al.*,<sup>12</sup> where these vortices grow in size while ascending upward and merges leading to the formation of puffs.

Coupling of two or more such candle-flame oscillators induces various coupled dynamics in the oscillations of their flames.<sup>8-10</sup> Among such coupled dynamics, synchronization is the phenomenon of adjustment of time scales of coupled oscillators to a common state due to the interaction between them.<sup>13</sup> The phenomenon of synchronization is ubiquitous in nature. It has been observed in various disciplines of science and engineering<sup>14-18</sup> since its discovery by Huygens.<sup>19</sup> When the coupling between the oscillators is weak, only locking of instantaneous phases of the oscillators take place. On the other hand, for a stronger form of coupling, the amplitudes of both the oscillators also exhibit a perfect locking. The basic requirements for the occurrence of synchronization are self-sustained oscillators and the existence of coupling between them. Candle-flame oscillator being self-sustained in nature when coupled with another such oscillator shows different modes of synchronization as the distance between them is gradually varied.

Kitahata *et al.*<sup>8</sup> discovered two modes of coupled behaviour in a pair of coupled candle-flame oscillators, namely in-phase and anti-phase synchronization when the distance between the oscillators is changed. In-phase synchronization is observed at small distances, whereas anti-phase synchronization occurs when the oscillators are sufficiently far apart. During in-phase synchronization, both flames attain maximum and minimum flame height, simultaneously. On the other hand, during the state of anti-phase synchronization, when one flame attains maximum flame height, other flame is at its minimum flame height. In addition to this, Manoj *et al.*<sup>10</sup> identified the state of amplitude death in between the known states of in-phase and anti-phase synchronization in such a system of oscillators. This state occurs at distances intermediate to that of in-phase and anti-phase synchronization. During the state of amplitude death, oscillations in both the flames cease and the flames attain a slender geometry. They noticed that the occurrence of amplitude death state is determined by the number of candles in each oscillator. Increasing the number of candles in each oscillator results in the reduction of the range of distances over which amplitude death is exhibited by these oscillators.

Furthermore, Manoj *et al.*<sup>10</sup> generalized the occurrence of different synchronization modes exhibited by two candle-flame oscillators to the coupled dynamics of a pair of Stuart-Landau (SL) oscillators. Coupling SL oscillators through time delay coupling alone, they showed the existence of similar dynamics (i.e., the presence of amplitude death between the states of in-phase and anti-phase synchronization) as observed in coupled candle-flame oscillators. In such a generalization, they related the distance between the

oscillators to time delay and the number of candles in an oscillator to coupling strength between the oscillators.

Another study by Okamoto *et al.*<sup>9</sup> presents different modes of coupled behaviour for a system of three coupled candle-flame oscillators. For such a system, four modes of coupled behaviour were observed: in-phase, partial in-phase, amplitude death and rotation mode. During partial in-phase mode, while two oscillators attain maximum height simultaneously, the third oscillator reaches its minimum flame height. All oscillators are synchronized during rotation mode; however with a constant phase difference of 60 degrees between them. Besides the studies on synchronization in candle-flame oscillators, the coupling of individual candle-flames kept in the vicinity of each other has also been studied. Forrester<sup>20</sup> observed various collective dynamics for an array of candle flames when the number and the position of individual candles in the array are changed. Their study highlights the cumulative effects arising due to the coupling of the candle flames such as synchronized arching and bowing of flame surfaces and enhancement/suppression of the central flame by the surrounding flames.

Various speculations regarding the occurrence of synchronization phenomena in a system of coupled candle-flame oscillators have been made. The study by Kitahata *et al.*<sup>8</sup> concluded that the synchronization between two candle-flame oscillators is a result of the interaction between the oscillators through thermal radiations. On the other hand, Okamoto *et al.*<sup>9</sup> suggested that the interactions of toroidal vortices formed around individual oscillators are responsible for this synchronization. Their study presumed that the relative positioning of vortices around the oscillators determines the occurrence of each mode of the coupled behaviour. The study by Yang *et al.*<sup>12</sup> ascribed the coupling of shear layers between two flames to cause in-phase and anti-phase synchronization modes. Manoj *et al.*<sup>10</sup> postulated the role played by time-delay coupling at various distances between the oscillators in inducing the coupled dynamics of candle-flame oscillators. Although these attempts have been made to explain the physical reasoning for the appearance of different modes of coupled behaviour in candle-flame oscillators, experimental evidence supporting these explanations is still unavailable in literature.

Thus, the objective of the present study is unravel the physical mechanism responsible for the occurrence of different modes of coupled behavior, i.e., in-phase synchronization, amplitude death, anti-phase synchronization, and desynchronization, exhibited by a pair of candle-flame oscillators through experiment. Towards this purpose, we investigate the flow field developed around the flames in both the oscillators using a shadowgraph imaging technique as the distance between these oscillators is changed. Simultaneous CH\* chemiluminescence images of the flames are also acquired to compare the flame dynamics with the flow dynamics. Distinctive characteristics of the surrounding flow field are seen during the occurrence of these modes in the system. We observe that the structure of vortices generated in the flow field and their self-organized positioning around the flames are the main factors responsible for the existence of different

coupled motions in the system of candle-flame oscillators. We also discuss the reason behind the change in the frequencies of oscillators during the transition from in-phase to anti-phase synchronization. The relation between the length scales (the vertical span of the vortex structure) and the timescales (vortex shedding frequencies) of vortices with the distance between the oscillators provides physical insight behind the change in the frequency of oscillations observed during the transition of coupled dynamics from in-phase to anti-phase state.

## II. EXPERIMENTAL SETUP

To study synchronization of two candle-flame oscillators, each oscillator is mounted on separate platforms (one fixed and the other movable) of a traverse system (refer Fig. 1a). Here candles, made of paraffin wax, having a cylindrical geometry with a height of 100 mm and a diameter of 8 mm are used. To make a candle-flame oscillator, four such candles are bundled together in such a way that their flames are merged to form a single compound flame. The center to center distance between the oscillators ( $d^*$ ) is changed by moving one platform with respect to the other. Here,  $d^*$  is increased from 18 mm to 38 mm in steps of 2 mm, and from then on up to 74 mm in steps of 3 mm. The value of  $d^*$  is non-dimensionalized using the diameter ( $D = 16$  mm) of an isolated oscillator (i.e.,  $d = d^*/D$ ). The lead screw of the traverse system has a least count of 0.5 mm. The whole system is raised 1 m from the ground to avoid ground effects on the oscillations of candle flames. The candles used for the experiments are long enough such that the flame location above the platform is sufficiently high at the end of the experiments, and thereby the effects of the platform on the buoyancy flows induced by the flames are neglected. The time scale associated with the regression rate of the candle wax is approximately 2.5 mm/min, and the total duration of the experiment is 660 s. The experiments were conducted under closed quiescent conditions such that any possibilities of external interferences were eliminated.

Simultaneous shadowgraph<sup>21</sup> and  $\text{CH}^*$  chemiluminescence imaging of the flames are performed to characterize the

coupled behaviour of candle-flame oscillators at various distances between them (refer Fig. 1b). Flame chemiluminescence imaging is used to describe the dynamics of the oscillating flames, while shadowgraph imaging is used to characterize the unsteady hydrodynamic flow field developed around each oscillator.<sup>22</sup> Other imaging techniques such as particle image velocimetry (PIV) cannot be used to do so, as the system is susceptible to external perturbations and the particle seeding used in such measurements would disturb the flame dynamics or can quench the oscillations of the flames.

As shown in Fig. 1b, the shadowgraph setup consists of a monochromatic light source, a pin-hole, a concave mirror, an imaging plane, and a camera. The light rays emanating from the source pass through the pin-hole, placed at the focal length of the mirror, and fall on the concave mirror. This produces a parallel beam of light which later falls on the imaging plane, after passing through the test section. The focal length and the aperture of the mirror are 100 cm and 20 cm, respectively, providing a sufficient range to capture the flame dynamics. The shadowgrams produced on a screen kept at a distance of 100 cm from the experimental setup are recorded using a Phantom V.12.1 high-speed camera (indicated in the figure as camera 1). The  $\text{CH}^*$  chemiluminescence images of the flames are captured using a Photron FASTCAM SA4 high-speed camera (indicated in the figure as camera 2) mounted with a  $\text{CH}^*$  filter (wavelength 435 nm and 10 nm full width at half maximum) on the lens. Chemiluminescence and shadowgraph images were simultaneously acquired at a frame rate of 250 fps by synchronizing both the cameras. A Tektronix AFG1022 function generator is used for concurrently triggering both cameras. Separate videos of flame chemiluminescence and shadowgraph (supplementary material videos S1 to S4) obtained during different states of coupled dynamics of candle flame oscillators are provided as supplementary material videos.

The data were acquired for a duration of 6 s for values of  $d^*$ . The oscillation frequency of an isolated candle-flame oscillator is around 11.1 Hz. We notice that the instability of the buoyancy induced flows around such oscillator results in the formation of a series of toroidal vortices at this frequency

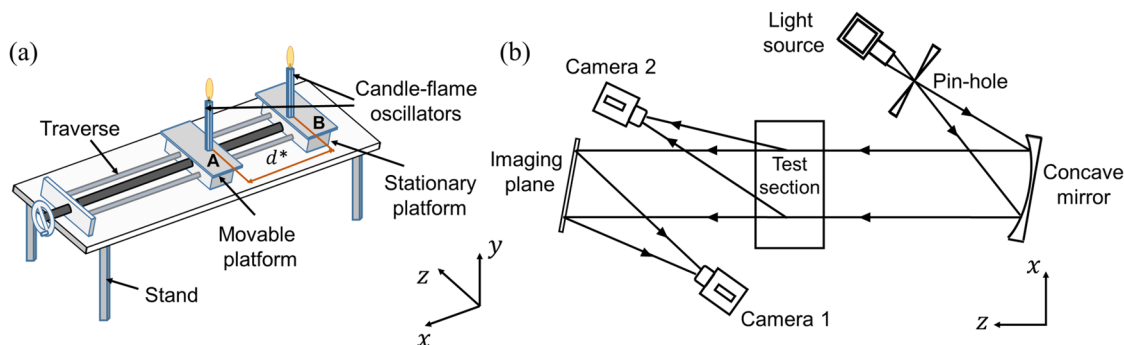


**FIG. 1.** (a) Schematic of the experimental setup used to study the coupled behaviour of two candle-flame oscillators (isometric view). One oscillator is mounted on a stationary platform B and the other on a movable platform A of the traverse mechanism. The center to center distance ( $d^*$ ) between the oscillators is varied by moving the platform A against the platform B. (b) Diagram of shadowgraph imaging setup. Experimental setup shown in (a) is kept in the test section of (b).

encompassing the flame. The upward motion of such vortices produces self-sustained oscillations in the flame. Since the dynamics of two such oscillators are periodic (except during the amplitude death state), the sampling frequency (i.e., 250 Hz) and the total data length (i.e., 6 s) are sufficient to capture the asymptotic dynamical interactions exhibited by them at all distances ( $d^*$ ). To remove the transient effects and let the oscillators reach a steady state, a waiting time of 20 s was enforced after each increment in  $d^*$  prior to data collection. The instantaneous value of the flame chemiluminescence (or the heat release rate) at a particular value of  $d^*$  is constructed by summing up the intensity values of all pixels from the flame image of an individual oscillator. The same procedure is performed for successive frames of the video to obtain the time series of the heat release rate. The fluctuating heat release rate is obtained by subtracting the mean value from the instantaneous values of the time series.

### III. RESULTS AND DISCUSSIONS

In this section, we discuss the effect of the change in distance between two candle-flame oscillators ( $d$ ) on the response dynamics of their coupled interaction. We notice that with the change in  $d$ , the dynamics of these coupled oscillators exhibit four distinct modes, as previously reported by Manoj *et al.*<sup>10</sup> These modes include in-phase, amplitude death, anti-phase and desynchronized state of the oscillations. Shadowgraph imaging of the candle-flame oscillators helps to visualize the projection of the three-dimensional toroidal vortex on a two-dimensional plane as shown in Fig. 2. The periodic formation of these vortices surrounding the candle flames is

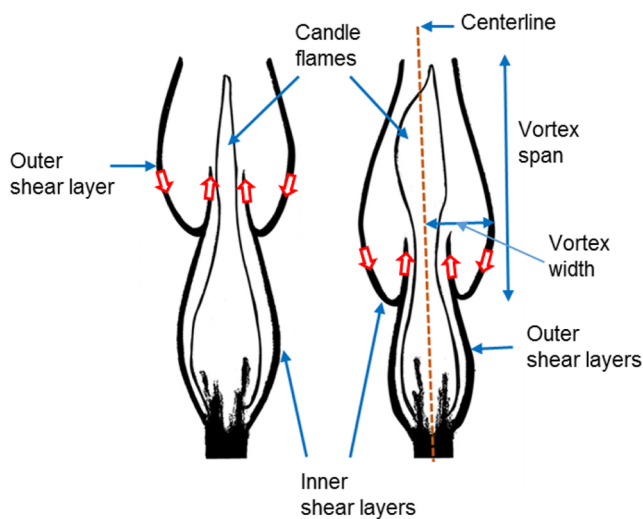


**FIG. 2.** Schematic of the binarized shadowgraph image of two candle-flame oscillators positioned at  $d = 3.87$  where they display desynchronized oscillations. The formation of vortices along the inner and outer shear layers surrounding the flames are shown by velocity vectors. The vortex span measures the height of the fully developed vortex, and the vortex width indicates the horizontal distance of the vortex boundary (inner or outer) from the central line of the oscillator.

due to the presence of buoyancy-induced Kelvin-Helmholtz instability.<sup>5,6</sup> The boundaries of such two-dimensional vortices are marked along the inner and outer shear layers of the oscillators. Here, the shear layers formed in the space between the oscillators are marked as the inner shear layers, whereas that exterior to the oscillators are marked as the outer shear layers. The roll-up of these unstable shear layers results in the formation of vortices around the flames. As the vortices move upwards, due to their self-induced velocity and the effects of buoyancy, they exhibit a growth in their shape as well as in size. The vertical span of each vortex ( $L^*$ ) is identified as the streamwise dimension of the vortical structure (indicated in Fig. 2 as the vortex span). This vertical span is measured when the amplitude of the flame oscillations is maximum. We further measure the velocity ( $u$ ) of these vortices, which is also the velocity of the buoyancy-induced flow, by tracking the displacement of the vortical structure in subsequent images of their oscillation cycle. In the following sections, we compare the essential features of the oscillatory flames and the interactions of the vortical structures formed around the flames during each mode of coupled dynamics of the oscillators.

#### A. Different modes of coupled dynamics observed in a pair of candle-flame oscillators

##### 1. In-phase synchronization

When two candle-flame oscillators are very close to each other, we notice in-phase mode of synchronization in their oscillations.<sup>8-10</sup> Such a state of oscillations is typically observed for  $d$  ranging from 1.13 to 1.5. The time series obtained from the  $\text{CH}^*$  chemiluminescence images of the flames for both the oscillators display nearly identical waveforms with a phase difference of approximately zero degrees (Fig. 3a), due to the resemblance in their flame dynamics. During each oscillation cycle (refer Fig. 3b), the luminous part of both the flames elongate simultaneously in the upward direction from their initial base state until a maximum flame height is attained. At this instance, a portion of the flame tip is cut off, which eventually turns into a puff of smoke. Later, both flames contract and come back to their initial state simultaneously. Besides this axial oscillatory motion, lateral deformation of the inner and the outer edges of the luminous flames is also observed (Fig. 3b). The outer edges of both the flames deform inwards during the elongation cycle and subsequently return to their initial position as the flames contract to reach their minimum height. On the contrary, inner edges exhibit minimal fluctuations and thus remain upright during each cycle of the candle-flame oscillations.

Figure 3c shows the sequence of shadowgraph images acquired over an oscillation cycle during the state of in-phase synchronization. Since the distance between the candle-flame oscillators is minimal, we observe the coalescence of two buoyancy-induced flows, especially along the inner shear layers (as marked in Fig. 2), generated around individual flames in these oscillators (refer Fig. 3c). However, the  $\text{CH}^*$  chemiluminescence images of the flames for both the oscillators show a small gap in between their inner edges, as observed from Fig. 3b. The merged buoyancy-induced flows act as a

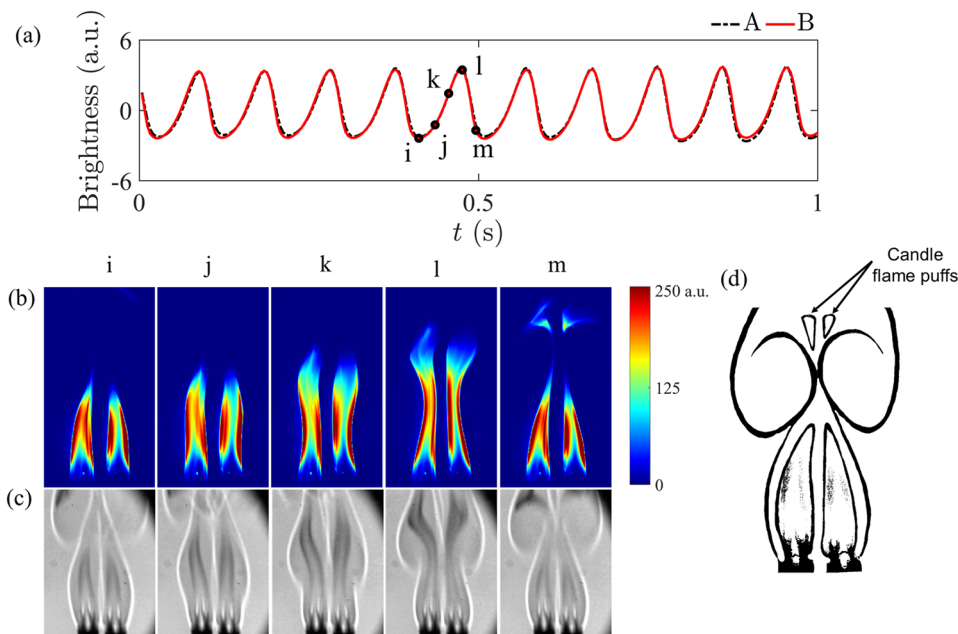


**FIG. 3.** (a) The times series of the total heat release rate obtained from the  $\text{CH}^*$  chemiluminescence images of individual candle-flame oscillators (A and B) during the state of in-phase synchronization ( $d = 1.25$ ). (b), (c) A sequence of the flame and the shadowgraph images, respectively, of the candle-flame oscillators corresponding to the time instances marked in (a) over an oscillation cycle. (d) A schematic of candle-flame oscillators (corresponding to the binarized shadowgraph image shown at the time instant 'm' in c), highlighting the interaction of the outer shear layers of both the oscillators causing the simultaneous formation of puffs in their flames.

single entity, wherein the synchronized symmetrical (or varicose) vortex shedding is observed along the outer shear layers of both the oscillators (refer Fig. 3d). The size of the vortices formed on the outer shear layers increases gradually as they move upwards. The interaction of these vortices with the flame surfaces induces various features in their flame geometry. While these vortices move upwards, they concurrently elongate the flame surfaces<sup>23,24</sup> until a maximum flame height is reached.

At this point, the size of such vortices is big enough to touch each other, thus causing the simultaneous pinching of edges of both the flame tips resulting in the formation of puffs (see Fig. 3d). Continuous formation and motion of such vortices cause repeated elongation and contraction in the flame surface, thereby inducing oscillations in the flame surfaces.

## 2. Amplitude death

On increasing the distance between the oscillators, we observe a cessation in the oscillations of both the oscillators

(see Fig. 4a). This phenomenon is referred to as amplitude death<sup>9,10</sup> and is observed for values of  $d$  ranging from 1.5 to 2.0. The time series of the total heat release rate of both the oscillators show only minimal aperiodic fluctuations (Fig. 4a), indicating their amplitude death behaviour. During this state, the flame shapes of both the oscillators exhibit an elongated slender geometry (Fig. 4b). The buoyancy-induced flows of individual candle-flame oscillators are no longer merged, and their inner shear layers are observed to be adjoined (Fig. 4c). Therefore, no substantial velocity gradient is created across the inner shear layers of the flow. As a result, the vortex formation along the inner shear layers ceases. This effect is then transferred to the outer shear layers, due to the toroidal nature of the vortices developed around the flames, causing the complete cessation of oscillations in the flame surfaces of both the oscillators (refer Fig. 4c). This characteristic of buoyancy-induced flows causing amplitude death in coupled candle-flame oscillators cannot be inferred from the flame images (Fig. 4b), where a larger gap is observed in between the inner flames.

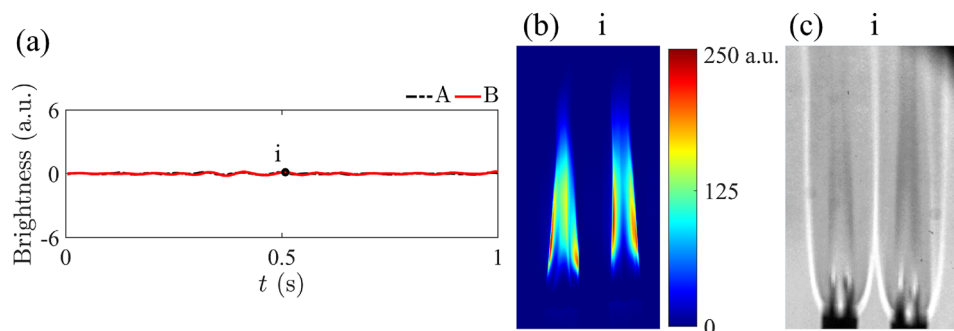


**FIG. 4.** (a) The times series of the total heat release rate obtained from the  $\text{CH}^*$  chemiluminescence images of individual candle-flame oscillators (A and B) during the state of amplitude death ( $d = 2.0$ ). (b), (c) The snapshots of the flame and the shadowgraph images, respectively, corresponding to the time instance marked in (a).

### 3. Anti-phase synchronization

With further increase in  $d$ , we observe that the flames regain their oscillatory behaviour from the amplitude death state in both the candle-flame oscillators; however, the oscillations now have a phase difference of 180 degrees (Fig. 5a). This state of oscillations is referred to as anti-phase synchronization.<sup>8,10</sup> The state of anti-phase synchronization occurs typically over values of  $d$  ranging from 2 to 3.31. The dynamics of the flames observed during this state is such that when one flame attains a maximum flame height and is about to release its puff, the other flame is at the position of its minimum flame height (Fig. 5b). We notice that such flame puff is formed due to the coalition between the boundaries of both inner and outer shear layer vortices of the same flame, shown in Fig. 5d. Contrary to our observation during in-phase synchronization, during the state of anti-phase synchronization, the inner edges of the flames exhibit periodic deformations, and their outer edges show minor fluctuations. Further, we note that even though both inner edges show an oscillatory behaviour, these surfaces always remain parallel to each other (Fig. 5b).

During the state of anti-phase synchronization, the distinct buoyancy-induced flows are observed around each oscillating flame, wherein vortex shedding takes place along both the outer and the inner shear layers (Fig. 5c). Here, we conjecture that although the space between two oscillators is sufficiently large for the formation of vortices, it is not large enough for the simultaneous accommodation of such vortices formed along the inner shear layers of the oscillators. As a result, the vortices are self-organized in such a way that the vortex formed around the flame of one oscillator is located above the vortex formed around the flame of another oscillator (refer Fig. 5c). This sinuous mode of vortex shedding

along the inner shear layers of the oscillators thus results in the alternate elongation and contraction of the flames. During this state, we observe that the vortices on the inner shear layers move slightly faster than the outer shear layers (refer to Figs. 5c-k to 5c-m). Asymmetry in the shape of the toroidal vortex can thus be attributed to the asymmetrical distribution of the vorticity. We conjecture that the inner side of the vortices experiences more flow velocity due to natural convection of hot surrounding air compared to the outer side which experiences lower flow velocity due to the cold ambient air. This leads to a difference in the vorticity of the inner side and the outer side, the vorticity of the former being larger than the latter. Hence, if the circulation of the toroidal vortex is a constant, the portion of the vortex along the inner side of the oscillator is wider (i.e., the larger value of horizontal span measured from the center of each oscillator to the edge of the vortex) and therefore has larger curvature, as compared to the portion of the vortex along the outer side of the oscillator.

### 4. Desynchronization

When the distance between oscillators is increased further, we observe a disruption in the anti-phase synchronization motion of both the oscillators. We notice that the oscillations are uncorrelated and hence this particular state is referred to as desynchronization.<sup>10</sup> Typically, this state is observed for  $d$  larger than 3.31. The time series of the total heat release rate obtained from the  $\text{CH}^*$  chemiluminescence images of individual candle-flame oscillators do not exhibit identical waveforms (Fig. 6a), and also the relative phase difference between them changes with time. This is in contrast with the behaviour observed during the states of in-phase and anti-phase synchronization where the time series of the total

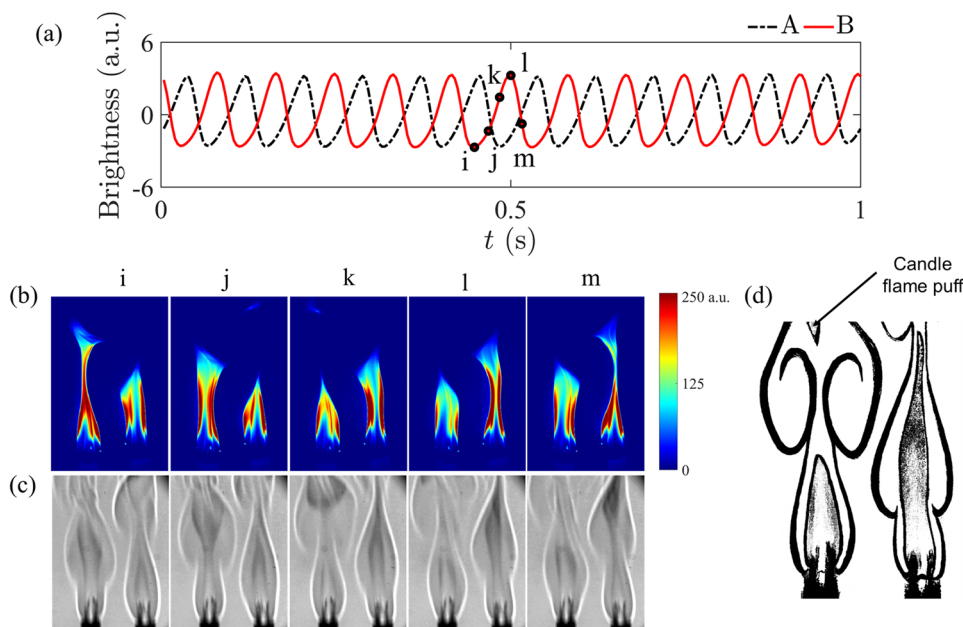


**FIG. 5.** (a) The times series of the total heat release rate obtained from the  $\text{CH}^*$  chemiluminescence images of individual candle-flame oscillators (A and B) during the state of anti-phase synchronization ( $d = 2.37$ ). (b), (c) A sequence of the  $\text{CH}^*$  chemiluminescence of the flame and the shadowgraph images, respectively, corresponding to the time instances marked in (a) over an oscillation cycle. (d) A schematic of candle-flame oscillators (corresponding to the binarized shadowgraph image shown at the time instant 'k' in c), highlighting the interaction of inner and outer shear layers of one of the oscillators resulting in the formation of a puff while the other oscillator reaches its maximum height. The self-adjustment of the vortices on the inner shear layers of both the oscillators is also seen in (d).

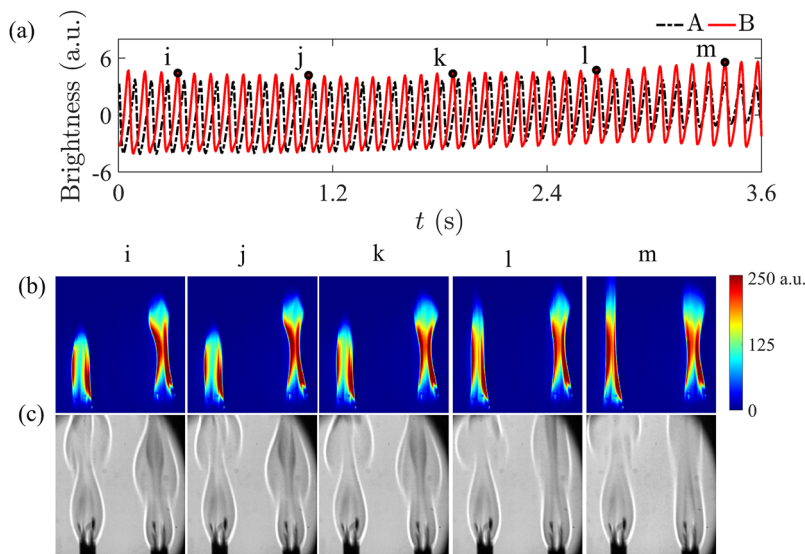


**FIG. 6.** (a) The times series of the total heat release rate obtained from the  $\text{CH}^*$  chemiluminescence images of individual candle-flame oscillators (A and B) during the state of desynchronization ( $d = 3.87$ ). (b), (c) A sequence of the flame and the shadowgraph images, respectively, corresponding to the time instances marked in (a).

heat release rate of both the oscillators display a nearly identical waveform and also a constant instantaneous phase difference. As the interaction between the oscillators is reduced during the state of desynchronization, we further note that the attainment of maximum flame height during their oscillations is seemingly irregular (see Figs. 6a,b).

Contrary to the behaviour observed during the state of anti-phase synchronization, during desynchronization, the space between the two oscillators is sufficiently large for the simultaneous accommodation of vortices formed along the inner shear layers of both the oscillators (Fig. 6c). For each candle-flame oscillator, we notice the independent formation of vortices around their flames, which move upward without much influence from their neighbour. As a result, we observe independent oscillations in both the flames. Thus, our experiments suggest that the interactions of the vortices formed around the flames in the candle-flame oscillators play an essential role in determining the mode of their coupled dynamics.

### B. Variation in the vortex length scale and timescale with the distance between the oscillators

Various measures from synchronization theory can be used to characterize the dynamics observed in a pair of coupled candle-flame oscillators. Figure 7a shows the variation of the time-averaged value of the absolute relative phase  $|\Delta\Phi|$  between the pair of coupled candle-flame oscillators as the distance between them is varied. The different states of coupled dynamics observed in our system is demarcated in the plot. As discussed earlier, both the oscillators exhibit in-phase mode of synchronization, where  $|\Delta\Phi|$  is nearly equal to 0 degrees, for values of  $d$  in the range of 1.13 to 1.5. The state of anti-phase synchronization of oscillators is observed over a range of  $d$  from 2 to 3.31 with  $|\Delta\Phi|$  equal to 180 degrees. During the state of amplitude death, which occurs intermediary

to in-phase and anti-phase synchronization ( $1.5 \leq d \leq 2.0$ ), the Hilbert phase is undefined and is therefore not shown in the plot. During desynchronization ( $d > 3.31$ ),  $|\Delta\Phi|$  takes on random values in between 0 to 180 degrees.

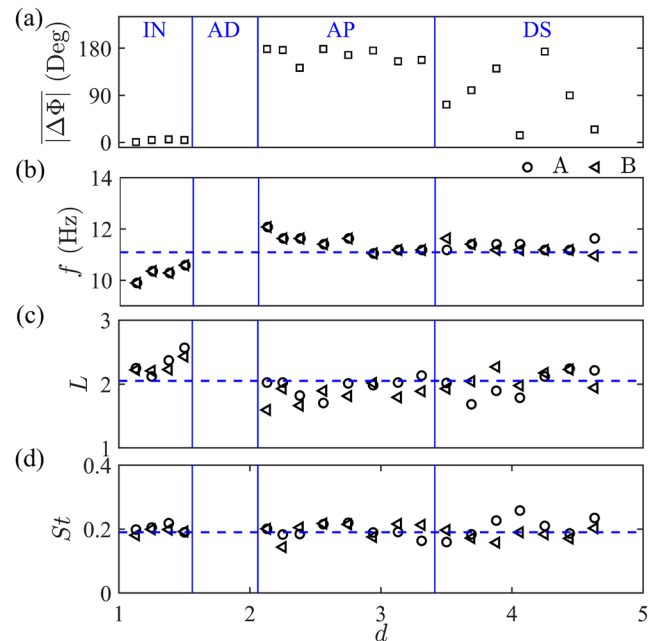


**FIG. 7.** Variation of (a) mean relative phase difference ( $|\Delta\Phi|$ ), (b) vortex shedding frequency ( $f$ ), (c) length scales ( $L$ ) of vortices, and (d) Strouhal number ( $St$ ) for a pair of coupled candle-flame oscillators (named as A and B) with  $d$ . Here, the regions of in-phase (IP), amplitude death (AD), anti-phase (AP) and desynchronization (DS) are marked separately. Horizontal broken line in (b)-(d) represents the frequency, length scales and Strouhal number, respectively, for an isolated candle-flame oscillator.

Finally, we try to characterize the variation in the properties of the vortices generated around each candle-flame oscillator as the distance between them is varied. Figures 7b,c show the variation of the vortex shedding frequency ( $f$ ) and the vertical span (length scale,  $L^*$ ) of the vortices (refer to Fig. 2) with the distance between the pair of candle-flame oscillators, respectively. Here,  $L^*$  is non-dimensionalized using the diameter ( $D = 16$  mm) of an oscillator (i.e.,  $L = L^*/D$ ) and has an uncertainty of  $\pm 0.25$  mm/pixel. We further express the properties of vortex shedding around the flame in terms of a non-dimensional number, the Strouhal number ( $St$ ), defined as follows:

$$St = \frac{fD}{u}$$

where  $f$  is the vortex shedding frequency,  $D$  is the diameter of a single oscillator, and  $u$  is the velocity of the vortices. We observe that the oscillation frequencies of both the flames are directly related to the frequency of vortex shedding around them, and the values of  $L$  are nearly the same for both the oscillators during each state of their coupled behaviour.

We notice a drop in the frequencies of both candle-flame oscillators during the state of in-phase synchronization, as compared to the frequency of an isolated candle-flame oscillator (shown by the dotted horizontal line in the Fig. 7b). On the other hand, a significant jump in the frequencies of both the oscillators as compared to their uncoupled frequencies is observed during the state of anti-phase synchronization.<sup>8,10</sup> The value of  $L$  is larger during the state of in-phase synchronization as compared to that of anti-phase synchronization. This observation suggests that, for smaller values of  $d$ , the buoyancy-induced flows around the flames in both the oscillators amalgamate and vortices are shed encompassing these flames. Such behavior of the vortex shedding further increases the span of the vortices by lowering their frequency of oscillations during the in-phase state of synchronization. In the case of anti-phase synchronization, the value of  $L$  is smaller, resulting in a faster shedding of vortices from both the oscillators.

During the transition of oscillators from anti-phase to desynchronized state, we observe a gradual increase in the vertical span of vortices, which is an affirmation of the decrease in the frequency of oscillations in both the flames with the increase in  $d$ . This decrease in frequency continues till the desynchronized state is reached where flame oscillations in both the oscillators become independent of each other. The frequency of oscillators during the state of desynchronization is observed to be approximately the same as the frequency of an isolated candle-flame oscillator. Hence, we conclude that a decrease in the length scales of vortices shed around the flames facilitates an increase in the frequency of oscillations during the transition from in-phase to anti-phase synchronization. Further, the Strouhal number for both candle flame oscillators is observed to be approximately equal to 0.2 for the entire range of  $d$  considered (Fig. 7d). Such a value of Strouhal number is typically associated with the low-frequency mode of vortex shedding occurring due to the large-scale instability of the shear layer.<sup>6</sup>

#### IV. CONCLUSIONS

The present study elucidates the physical reason behind the exhibition of the recently discovered four distinct dynamical states such as in-phase synchronization, amplitude death, anti-phase synchronization, and desynchronization in a pair of coupled candle-flame oscillators as the distance between them is varied. Using simultaneous measurements of shadowgraph and  $CH^*$  chemiluminescence imaging, we observe that toroidal vortices are formed surrounding the flames due to the instability of the buoyancy-induced flows. Upward motions of these vortices induce oscillations in the flames. Further, we note that the interaction between these vortices plays an essential role in determining the particular mode of the coupled behaviour in a pair of candle-flame oscillators. We observe the merging of the buoyancy-induced flows along the inner shear layers of both the flames during the state of in-phase synchronization, wherein the varicose mode of vortex shedding occurs only along the outer shear layers of oscillators. Increasing the distance between the oscillators separates the buoyancy-induced flows of each oscillator and the system transitions to exhibit amplitude death where vortex shedding ceases as their inner shear layers are adjoined. During the state of anti-phase synchronization, distinct vortices are formed along the outer as well as the inner shear layers, in which the inner vortices are observed to display a sinusoidal mode of vortex shedding. The state of desynchronization occurs for large distances between the oscillators where we notice independent formation and motion of vortices around the flames.

Furthermore, we identified the relation of vortex shedding frequency with the vertical span of the vortex. We observe that the decrease in the vertical span of the vortices results in more frequent shedding of vortices that, in turn, causes a sudden increase in the frequency of oscillations as the mode of synchronization changes from in-phase to anti-phase oscillations. Our current analysis on the interaction of coupled diffusion flames has possible implications in studying the dynamics of multiple flames observed in practical combustion systems such as household burners, gas turbine engines and rocket engines.

#### SUPPLEMENTARY MATERIAL

The simultaneous videos of  $CH^*$  chemiluminescence and shadowgraph of candle-flame oscillators obtained during the states of in-phase synchronization, amplitude death, anti-phase synchronization and desynchronization are provided as [supplementary material](#) videos S1 to S4, respectively.

#### ACKNOWLEDGMENTS

This work is supported by ONRG, USA (Contract Manager: Dr. R. Kolar, Grant No.: N62909-18-1-2061). We would like to thank Dr. G. Rajesh from the Department of Aerospace Engineering at IIT Madras for providing facilities to perform shadowgraph imaging. The support of Mr. Anil K. and Mr. Manikandan R. (IIT Madras) while performing experiments is gratefully acknowledged.

## REFERENCES

- <sup>1</sup>D. F. G. Durao and J. H. Whitelaw, "Instantaneous velocity and temperature measurements in oscillating diffusion flames," *Proc. R. Soc. Lond. A* **338**, 479–501 (1974).
- <sup>2</sup>A. J. Grant and J. M. Jones, "Low-frequency diffusion flame oscillations," *Combustion and Flame* **25**, 153–160 (1975).
- <sup>3</sup>T. Maxworthy, "The flickering candle: Transition to a global oscillation in a thermal plume," *Journal of Fluid Mechanics* **390**, 297–323 (1999).
- <sup>4</sup>S. Ghosh, S. Mondal, T. Mondal, A. Mukhopadhyay, and S. Sen, "Dynamic characterization of candle flame," *International Journal of Spray and Combustion Dynamics* **2**, 267–284 (2010).
- <sup>5</sup>J. Buckmaster and N. Peters, "The infinite candle and its stability—A paradigm for flickering diffusion flames," *Symposium (International) on Combustion* **21**, 1829–1836 (1988), Elsevier.
- <sup>6</sup>L. D. Chen, J. P. Seaba, W. M. Roquemore, and L. P. Goss, "Buoyant diffusion flames," *Symposium (International) on Combustion* **22**, 677–684 (1989), Elsevier.
- <sup>7</sup>M. Faraday, *The chemical history of a candle* (Barnes & Noble Publishing, 2005).
- <sup>8</sup>H. Kitahata, J. Taguchi, M. Nagayama, T. Sakurai, Y. Ikura, A. Osa, Y. Sumino, M. Tanaka, E. Yokoyama, and H. Miike, "Oscillation and synchronization in the combustion of candles," *The Journal of Physical Chemistry A* **113**, 8164–8168 (2009).
- <sup>9</sup>K. Okamoto, A. Kijima, Y. Umeno, and H. Shima, "Synchronization in flickering of three-coupled candle flames," *Scientific Reports* **6**, 36145 (2016).
- <sup>10</sup>K. Manoj, S. A. Pawar, and R. I. Sujith, "Experimental evidence of amplitude death and phase-flip bifurcation between in-phase and anti-phase synchronization," *Scientific Reports* **8**, 11626 (2018).
- <sup>11</sup>Y. Nagamine, K. Otaka, H. Zuiki, H. Miike, and A. Osa, "Mechanism of candle flame oscillation: Detection of descending flow above the candle flame," *Journal of the Physical Society of Japan* **86**, 074003 (2017).
- <sup>12</sup>T. Yang, X. Xia, and P. Zhang, "Anti-phase and in-phase flickering of dual pool flames," arXiv preprint [arXiv:1803.10411](https://arxiv.org/abs/1803.10411) (2018).
- <sup>13</sup>A. Pikovsky, M. Rosenblum, and J. Kurths, *Synchronization: A universal concept in nonlinear sciences*, Vol. 12 (Cambridge University Press, 2003).
- <sup>14</sup>A. T. Winfree, *The geometry of biological time*, Vol. 12 (Springer Science & Business Media, 2001).
- <sup>15</sup>Y. Kuramoto, *Chemical oscillations, waves, and turbulence* (Courier Corporation, 2003).
- <sup>16</sup>B. Blasius, A. Huppert, and L. Stone, "Complex dynamics and phase synchronization in spatially extended ecological systems," *Nature* **399**, 354 (1999).
- <sup>17</sup>L. Glass, "Synchronization and rhythmic processes in physiology," *Nature* **410**, 277 (2001).
- <sup>18</sup>S. Strogatz, *Sync: The emerging science of spontaneous order* (Penguin UK, 2004).
- <sup>19</sup>C. Huygens, 1665, Letter to de Sluse, *Oeuvres Completes de Christian Huygens* (letters).
- <sup>20</sup>D. M. Forrester, "Arrays of coupled chemical oscillators," *Scientific Reports* **5**, 16994 (2015).
- <sup>21</sup>G. S. Settles, *Schlieren and shadowgraph techniques: Visualizing phenomena in transparent media* (Springer Science & Business Media, 2012).
- <sup>22</sup>B. W. Albers and A. K. Agrawal, "Schlieren analysis of an oscillating gas-jet diffusion flame," *Combustion and Flame* **119**, 84–94 (1999).
- <sup>23</sup>W. M. Roquemore, L. D. Chen, J. P. Seaba, P. S. Tschen, L. P. Goss, and D. D. Trump, "Jet diffusion flame transition to turbulence," *The Physics of Fluids* **30**, 2600 (1987).
- <sup>24</sup>V. R. Katta and W. M. Roquemore, "Role of inner and outer structures in transitional jet diffusion flame," *Combustion and Flame* **92**, 274–282 (1993).